

# Accurate reference for shallow water bathymetry using a tilt-compensating dual-prism pole and time-synchronized robotic total stations

Lucas Dammert<sup>1</sup>, Jan Rhomberg-Kauert<sup>1</sup>, Tomas Thalmann<sup>1</sup>, Laure-Anne Gueguen<sup>1</sup>, David Monetti<sup>2</sup>, Hans-Berndt Neuner<sup>1</sup>  
and Gottfried Mandlbürger<sup>1</sup>

<sup>1</sup>Department of Geodesy and Geoinformation, TU Wien; 1040 Vienna, Austria - lucas.dammert@geo.tuwien.ac.at,  
jan.rhomberg-kauert@geo.tuwien.ac.at, laure-anne.gueguen@geo.tuwien.ac.at,  
tomas.thalmann@geo.tuwien.ac.at, hans.neuner@geo.tuwien.ac.at, gottfried.mandlbuerger@geo.tuwien.ac.at

<sup>2</sup>Skyability GmbH; GZO-Dienstleistungszentrum 5, 7011 Siegendorf, Austria - david.monetti@skyability.com,

**Keywords:** laser bathymetry, referencing, multibeam, SONAR, LiDAR, ground truth

## Abstract

Accurate and reliable reference data are key elements for advancing remote sensing techniques and validating the quality of geo data. This includes remote sensing methods for bathymetric data collection, such as SONAR or bathymetric LiDAR. In this work, we present a method for acquiring accurate bathymetric reference data for shallow water depths. We use a tilt-compensating dual-prism measurement pole combined with two time-synchronized robotic total stations to allow tilted and non-static pole measurements. The accessible water depth of our method is restricted only by the pole length. The error induced by pole tilt and movement, caused by water currents, large water depths, or the operation from unstable vehicles, is minimized by using the time-synchronized tilt information gathered from two reflectors mounted on the measurement pole. With our approach, we show in an air-only experiment that we achieve better than 1 cm height RMSE and 8 cm position RMSE for tilted measurement with a 4.65 m long pole. The variance propagation and precision values derived from our in-water study suggest an even lower position RMSE of 3 cm.

## 1. Introduction

Remote sensing methods for bathymetric data acquisition, e.g. LiDAR (Light Detection and Ranging) or SONAR (Sound Navigation and Ranging), are rapidly progressing in accuracy and availability (Mandlbürger, 2022). Automated platforms, such as unmanned surface vehicles (USVs) and unmanned aerial vehicles (UAVs), make SONAR and LiDAR sensors available at comparable low costs, together with high flexibility in use. On the manufacturer's side, both techniques achieve ranging accuracies of 1 cm to 2 cm (Riegl Laser Measurement Systems GmbH, 2021; Norbit Subsea, 2021; Leica Geosystems AG, 2025). To validate these accuracy claims, and obtain correct stochastic models for specific use cases, e.g., in the context of sensor integration and utilizing point cloud correspondences for trajectory estimation, a critical accuracy assessment of the bathymetric data is necessary. For bathymetric data, the total vertical uncertainty (TVU) requirements are usually higher than the total horizontal uncertainty (THU). Using the example of the IHO Exclusive Order, the TVU needs to be about 5 to 6 times more accurate than the THU for water depths of less than 10 m (International Hydrographic Organization, 2022). For nadir-looking measurements of SONAR or LiDAR, the TVU is mainly influenced by the ranging accuracy of the sensor. When considering the ranging accuracy of the sensors, a proper reference must outperform the specifications of the evaluated sensors. Thus, a sub-cm-accurate height reference for the bathymetric points is required.

For very shallow water with moderate flow velocities of less than 1.5 m water depth (i.e. wadeable water), a robotic total station (RTS) in combination with a measurement pole is a well-established reference tool (Bangen et al., 2014), as the water body is accessible for personnel. The RTS allows accurate height information at a low millimetre accuracy level (Leica Geosystems AG, 2016). However, the evaluation of LiDAR

and SONAR sensors in the event of strong currents and non-wadeable water depths of more than 1.5 m remains a challenge. Since depth-dependent uncertainties and scaling errors can best be identified in deeper waters and the accuracy of remote sensing techniques needs to be verified throughout the water penetration range, reference data are required for water depths greater than 1.5 m. To acquire these data, a boat or a comparable platform must be used to access survey locations. Similarly to strong currents, the boat greatly increases the difficulty in holding the measurement pole vertically above a ground point, as its momentum, the water current, and wind make stabilizing the boat over the survey location nearly impossible. In reality, the measurement pole might be fixed on a ground point, but the pole top moves together with the surveyor, making an accurate, conventional measurement infeasible. Especially in light of water depths and pole lengths exceeding well beyond 2 m, the height error introduced by even slight inclinations of the measurement pole quickly reaches several cm. The position error is even more sensitive to the pole inclination, easily reaching the dm-level.

In our study, we present a tilt-compensating dual-prism pole that allows the acquisition of bathymetric reference data while being tilted and moving (see Figure 1). This pole makes use of two time-synchronized RTS to measure the position of both prisms for a short period of time. Thus, the measured tilt vector of the pole can be used to propagate the measured reflector position onto the ground point, resulting in a time series of ground point coordinates eliminating the error introduced by pole movement or instability, as well as pole inclination. By introducing averaging over the time series, an accurate coordinate for the bathymetric reference point can be determined. Our method is generally usable for all environments but is restricted by practical limitations such as measurement pole length, which can reach lengths of 20 m, measurement range, line-of-

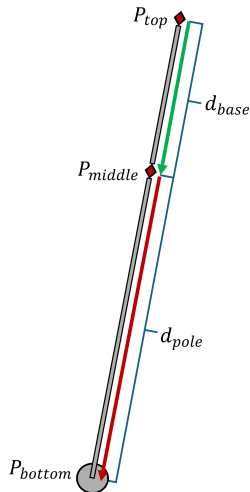


Figure 1. Sketch of the dual-prism pole.  $P_{top}$ ,  $P_{middle}$ ,  $d_{base}$ , and  $d_{pole}$  are known, thus, the green vector is determined and using the red vector  $P_{bottom}$  can be calculated.

sight between RTS and pole, and water velocity, which needs to allow a vessel to access the water body and must not significantly deform the pole.

Compared to existing IMU-based tilt-compensating poles (Maar, 2022; Thalmann and Neuner, 2024), our approach has two main advantages. Firstly, it does not include electronic components on the measurement pole, resulting in complete waterproofness of the pole. Secondly, no communication between the pole and the measurement instrument (RTS) is required. An additional advantage is that the necessary equipment, consisting of two RTS units and two prisms, is usually already available in surveying offices and research institutes, whereas IMU-based tilt-compensating solutions are less present. In this contribution, we present the theoretical basis on which this system is built (Section 3), perform a theoretical and experimental uncertainty evaluation (Section 4) and show insights from a field study (Section 4.3). Finally, we assess the suitability of our system for the collection of bathymetric ground truth data (Section 5).

## 2. Related Work

Bathymetric reference measurements can be characterized by the large negative height difference between accessible height above water, water surface, and point of interest at the bottom of the water body. This resembles the well-known surveying situation of a dual-prism measuring rod for sewer surveying. As the large pole length and limited accessibility make vertical alignment of the pole challenging, the inclination of the measurement pole is determined using measurements towards two prisms mounted on the pole, and the measured 3D coordinates are corrected. As this concept is well-established in surveying, the novelty of our contribution is not the prism-based tilt compensation itself but the extension of the channel staff concept with kinematic tracking capabilities and its adaptation for bathymetric reference measurements, as well as the evaluation of the system's uncertainty. Research on bathymetric ground truth with cm-accuracy for non-wadeable water depths is sparse. For wadeable waters, shallower than 1.5 m,

direct measurements with GNSS or RTS are common (Bangen et al., 2014) and thus accuracies of several millimetres can be reached. For non-wadeable waters, those techniques are also used with long measurement poles in combination with water surface vessels, but often lead to large uncertainties due to the pole movement and inclination. In Menna et al. (2024), pressure sensors are used to derive accurate height information as reference. Although this approach seems very promising, it requires additional measurement systems to obtain position information. IMU-based tilt-compensating measurement systems exist for GNSS receivers (Luo et al., 2018a; Trimble Inc, 2024; Luo et al., 2018b) and RTS applications (Maar, 2022; Thalmann and Neuner, 2024). In general, those systems are suitable for the acquisition of bathymetric reference data for large water depths and from moving vessels, as they address the major error sources of pole inclination and time synchronization for moving poles. However, the high level of electronic components and the high cost of these systems make their use for gathering bathymetric ground truth data difficult. For example, the commercially available IMU-based tilt-compensating measurement pole from Leica (Maar, 2022), relies on automatic height readings of the measurement pole. This makes the system unsuitable for extended use underwater. Scientific approaches like Thalmann and Neuner (2024) require a large amount of expertise to replicate both the hardware and the algorithmic solution. In contrast, the vertical uncertainty of GNSS-RTK receivers of more than 2 cm (Luo et al., 2018b; Trimble Inc, 2024; Wiener Netze GmbH & Co KG, 2024) makes them unsuitable for the collection of highly accurate bathymetric reference data.

The tilt-compensating dual-prism pole developed in our study leverages accurate RTS measurements together with a tilt-compensating technique based on the simultaneous measurement of two  $360^\circ$  mini prisms by two time-synchronized RTS. This approach relies on an accurate relative time synchronization between the two RTS, which has been extensively studied in Gojcic et al. (2018); Thalmann and Neuner (2021), and is comparably easy to replicate. In addition, our dual-prism pole makes use of major advancements in automated target recognition and tracking of the reflector by Leica RTS (Grimm and Hornung, 2015; Grimm et al., 2015). Consequently, our study and its results are limited to Leica RTS. In general, the observation of the dual-prism pole with two RTS faces a major challenge. Normally, the Automated Target Recognition (ATR) of the RTS identifies the correct reflector using the intensity of a laser pulse reflected by the prism (Grimm and Hornung, 2015). In our scenario, two reflectors exist within the field of view of the RTS, increasing the difficulty of correct reflector identification. Although this challenge is well compensated for additional static reflectors (Grimm and Hornung, 2015), the robustness against moving reflectors is harder to achieve. Our evaluation shows that this fact greatly reduces the achievable measurement distance to about 150 m, while also introducing an error quota caused by prism mix-ups of the two RTS. However, our investigation shows that no negative impact on the overall accuracy can be observed.

## 3. Method

The concept of our dual-prism pole is illustrated in Figure 1. It shows a measurement pole which has two prisms mounted on top, separated by a vertical extension. In our test, the two prisms  $P_{top}$  and  $P_{middle}$  are spaced 1.2 m apart, and the usable pole length  $d_{pole}$  can extend from 1.65 m to 4.65 m.

### 3.1 Time-synchronized RTS measurements

Each of the two prisms is observed by an RTS. In our study, we use two Leica MS60 (Leica Geosystems AG, 2016) featuring a measurement frequency of about 20 Hz. The RTS are time-synchronized using a joint controller, in our case, a Raspberry Pi 4. The measurements are performed using a serial connection and the GeoCom interface of the Leica RTS. The controller timestamps the received measurements, which transfers the measurements of both RTS into a common time frame. To estimate a linear model between the controller time and the RTS' own time system, a sensorboard calibration is performed in the field (Thalmann and Neuner, 2021). These timestamps must then be corrected for the latency of the RTS system, which is known from a laboratory calibration (Thalmann and Neuner, 2021). The methodology employed in our work is similar to Thalmann and Neuner (2021), with the exception that no absolute time reference is needed. Thus, only a relative time synchronization between both RTS is required, reducing the setup by one component, namely the GNSS receiver, which usually shares the pulse-per-second (PPS) signal with the controller for absolute time synchronization to GPS time. The absolute time synchronization would then allow the RTS observation to be used together with spatially distributed sensors, which are also synchronized to GPS time, like LiDAR or SONAR (Tombrink et al., 2023). It is important to note that while the Leica MS60 exhibits a non-significant delay between distance and angle measurements, other RTS models would require the correction of this so-called intrinsic latency (Thalmann and Neuner, 2021; Stempfhuber and Sukale, 2017). Additionally, the exhibited system latency of the RTS can be assumed to be similar for identical RTS configurations (hardware and firmware), which then has no effect on the measurement result. In our field tests, the velocity of the reflector was rather small, with the median speed being  $0.3 \text{ m s}^{-1}$  and 95% of the individual measurements occurring at a speed smaller than  $1 \text{ m s}^{-1}$ . Thus, even a latency difference of 10 ms, which is more than 10% of the exhibited latency of Leica RTS, would only lead to a positional error of 1 cm and a much smaller height error of 1 mm, as the vertical velocity is close to zero. This allows us to omit a precise temporal calibration of the RTS in a laboratory setup (Thalmann and Neuner, 2021), drastically reducing the effort to construct our system. Thus, for our study, the time synchronization is achieved only by timestamping the recorded RTS measurements. To allow a reliable measurement, we perform continuous, time-synchronized measurements of both prisms for about 10 s, resulting in about 200 individual measurements per prism. This time series of measurements allows for deriving an average position of the bathymetric reference point and obtaining statistical information about the quality of each measurement (see Section 4).

### 3.2 Tilt compensation

Having measured the 3D coordinates of both prisms ( $P_{\text{top}}(i)$  and  $P_{\text{middle}}(i)$ ) over the 10 s time window, they are used to determine the tilt vector  $d_{\text{base}}(i)$  (green arrow in Figure 1) over time. Using the known pole length  $d_{\text{pole}}$  (red arrow in Figure 1), the bottom point ( $P_{\text{bottom}}(i)$ ) can be calculated for each measurement pair  $i$  in the time window. The mathematical relation between the measured points and the bottom point is given by:

$$d_{\text{base}}(i) = \frac{P_{\text{bottom}}(i) - P_{\text{top}}(i)}{\|P_{\text{bottom}}(i) - P_{\text{top}}(i)\|} \quad (1)$$

$$P_{\text{bottom}}(i) = P_{\text{middle}}(i) + d_{\text{base}}(i) \cdot d_{\text{pole}} \quad (2)$$

Following the assumption that the foot of the pole is static throughout the measurement time, the  $n$  measurements can be averaged, resulting in the mean bottom coordinate  $\bar{P}_{\text{bottom}}$ . In addition, the corresponding standard deviation of each coordinate component  $s(P_{\text{bottom}})$  can be calculated and provides a precision measure for each point.

$$\bar{P}_{\text{bottom}} = \frac{1}{n} \sum_{i=1}^n P_{\text{bottom}}(i) \quad (3)$$

$$s(P_{\text{bottom}}) = \sqrt{\frac{1}{n} \sum_{i=1}^n (P_{\text{bottom}}(i) - \bar{P}_{\text{bottom}})^2} \quad (4)$$

## 4. Evaluation

To evaluate the proposed dual-prism pole, we perform a theoretical variance propagation and an experimental evaluation. During the experimental evaluation, the pole is surrounded by air, and a reference coordinate of the pole bottom is known. We also perform a field test in which the pole is used in real conditions, which means that the pole is completely submerged in water. However, for the field test, we do not have reference data.

### 4.1 Variance propagation

With the pole length and baseline between both prisms defined and the measurement uncertainty of RTS well studied (Thalmann and Neuner, 2021; Vogel et al., 2023; Kälin et al., 2022), we can perform a variance propagation based on Equations 1 and 2:

$$\sigma(P_{\text{bottom}}) = \sqrt{\begin{aligned} &\left(1 + \frac{d_{\text{pole}}}{d_{\text{base}}}\right)^2 \sigma(P_{\text{middle}})^2 + \left(-\frac{d_{\text{pole}}}{d_{\text{base}}}\right)^2 \sigma(P_{\text{top}})^2 \\ &+ \left(\frac{P_{\text{middle}} - P_{\text{top}}}{d_{\text{base}}}\right)^2 \sigma(d_{\text{pole}})^2 \\ &+ \left(-\frac{(P_{\text{middle}} - P_{\text{top}})d_{\text{pole}}}{d_{\text{base}}^2}\right)^2 \sigma(d_{\text{base}})^2 \end{aligned}} \quad (5)$$

Based on the uncertainty information from the RTS data sheet (Leica Geosystems AG, 2016) and Thalmann and Neuner (2021), we assume a standard deviation for RTS measuring the kinematic prisms of about  $\sigma(P_{\text{top}}) = \sigma(P_{\text{bottom}}) = 3 \text{ mm}$ . The uncertainty introduced by the geometric transformation between both RTS can be assumed to be smaller than 1 mm, if a sufficient number of points are used for the transformation. Thus, this influence is neglected in our assessment. In addition, the measurement pole length as well as the baseline between both prisms can be accurately measured in the field using the RTS or calibrated in a laboratory environment, leading to standard deviations of at most  $\sigma(d_{\text{base}}) = \sigma(d_{\text{pole}}) = 1 \text{ mm}$ .

Following Equation 5, this results in a standard deviation vector for the measured bottom point of  $\sigma(P_{\text{bottom}}) = [18, 18, 19] \text{ mm}$  if the whole pole length of 4.65 m is used. With decreasing pole length, the uncertainty also decreases. The relation is roughly linearly proportional, leading to an uncertainty vector of  $\sigma(P_{\text{bottom}}) = [12, 12, 12] \text{ mm}$  at a pole length of 2.65 m.

This variance propagation is limited to the bottom point coordinate in a local coordinate frame. For the transformation into a superior coordinate system, e.g. WGS84 UTM 33N, an additional uncertainty by the coordinate transformation is introduced. This uncertainty varies with the transformation strategy used. Although static GNSS observations can achieve transformation uncertainties at the low millimetre level, RTK-based measurements can easily yield errors of several centimetres. However, for accurate measurement tasks, the local coordinate system might be of greater interest. Using reference objects, e.g. geometric planes, or point cloud matching strategies, the accurate transformation between LiDAR point clouds and terrestrial reference data is possible.

## 4.2 Experimental evaluation

To confirm the theoretically estimated uncertainty of the tilt-compensating dual-prism pole, we performed an experimental evaluation. This evaluation took place outdoors during sunny weather and the measurement distance was about 80 m, resulting in a quite realistic scenario. The biggest limitation is the non-submerged state of the pole, changing its movement characteristics. The pole is placed on a reference point with known coordinates. Then, the dual-prism measurement is performed for several minutes, and the bottom point is calculated. This is done with constant movement and thus change in inclination magnitudes and direction, as well as for different pole lengths (2.68 m, 3.68 m and 4.65 m). Due to constant movement, we simulate the behaviour during a measurement campaign on the water as well as possible and include the effects of moving water surface and pole vibrations caused by the pole movement in our evaluation. The inclination ranges from  $0^\circ$  up to  $30^\circ$ , similar to the data of our field test.

The first meaningful measure that can be derived is the distance variation  $d_{\text{pole}}$ , which gives a direct impression of the uncertainty of the measurement between the two RTS. The value  $d_{\text{pole}}$  is assumed constant, and every deviation from the calibrated value is the effect of the propagated measurement uncertainty and the uncertainty of the geometric transformation of both RTS. In our experiment, these deviations of the individual measurements have a root mean square error (RMSE) of 2 mm, 3 mm and 5 mm for the heights of 2.68 m, 3.68 m and 4.65 m. In general, this aligns well with the assumed standard deviations of the RTS measurement. However, for the full pole length of 4.65 m, the value is greater than for the rest, possibly indicating a deformation of the baseline segment.

The more significant value is the discrepancy between the reference point and the calculated pole bottom points. The discrepancies are shown as box plots in Figure 2. The left side of Figure 2 shows the discrepancies for the individual positions and the right side shows the discrepancies after averaging over 200 measurements, which corresponds to our 10 s measurement window. We see that the height is determined much more accurately before and after averaging. After averaging, the Inter-Quartile Range (IQR) is 4-5 times smaller than for the horizontal axes. Table 1 shows the respective RMSE values for po-

RMSE	Individual [cm]	Average [cm]	Average & Tilt Filter [cm]
Position (2.68 m)	7.9	3.3	2.9
Height (2.68 m)	1.4	1.4	0.7
Position (3.68 m)	14.0	5.0	5.0
Height (3.68 m)	2.3	0.6	0.7
Position (4.65 m)	15.9	8.4	8.9
Height (4.65 m)	2.7	1.6	0.9

Table 1. RMSE values for Euclidean position and height for individual measurements, after averaging over 200 measurements, and after additionally introducing a maximum tilt angle of  $15^\circ$  for all three investigated pole lengths.

sition and height observations for the different processing steps for all three investigated pole lengths. For the maximum pole length of 4.65 m, the (euclidean) position shows an RMSE of 15.9 cm for individual observations, which reduces to 8.4 cm when averaging over 200 measurements. For an individual height measurement with a pole length of 4.65 m, we observe an RMSE of 2.7 cm. After averaging, this value reduces to 1.6 cm. In addition, we see a strong correlation between pole length and measurement uncertainty. Furthermore, our investigation shows that shorter averaging windows also increase the RMSE, which means less accurate measurements. In general, we observe a correlation between the pole tilt and the measurement error. For example, by rejecting measurements with pole tilt angles larger than  $15^\circ$ , we improve the height RMSE to 0.9 cm after averaging (Table 1).

Figure 3 shows the differences of the individual measurements to the average value of each time window for the test with a pole length of 4.65 m; Figure 3 - Left for the vertical dimension and Figure 3 - Right for the horizontal dimension. This representation enables us to derive a precision value from the measurement itself, without relying on reference information, which can also be derived during real measurements. We use this distribution in Section 4.3 to compare the experimental evaluation and our field test. For the experimental evaluation, we see that, while the vertical component shows a distribution ranging roughly from  $-5 \text{ cm}$  to  $5 \text{ cm}$ , the x and y values range from  $-25 \text{ cm}$  to  $25 \text{ cm}$ . The standard deviations are 2 cm for the vertical and 16 cm for the euclidean horizontal component, which are similar magnitudes to the RMSE values calculated relative to the reference point before averaging. This suggests that the standard deviation of these differences can be used to estimate the RMSE of our measured coordinates. However, especially the horizontal standard deviation is higher than estimated in the variance propagation. We assume the deformation of the measurement pole to be the main reason.

## 4.3 Field test

In the field campaign, we acquired approximately 150 bathymetric ground points in different water bodies in the Pielach River region in Lower Austria (Figure 4). Our measurement setup, consisting of two RTS, a controller, and a measurement team in a canoe, is shown in Figure 5. This data set allows us to obtain several real-world results. Analogue to Figure 3, we can first determine the difference of an individual measurement, including the propagation to the pole bottom point relative to the mean pole bottom point, of each 10 s time window. Figure 6 shows this distribution of the differences between the individual measurements and the respective mean value for the vertical component (Left) and the two horizontal components (Right).

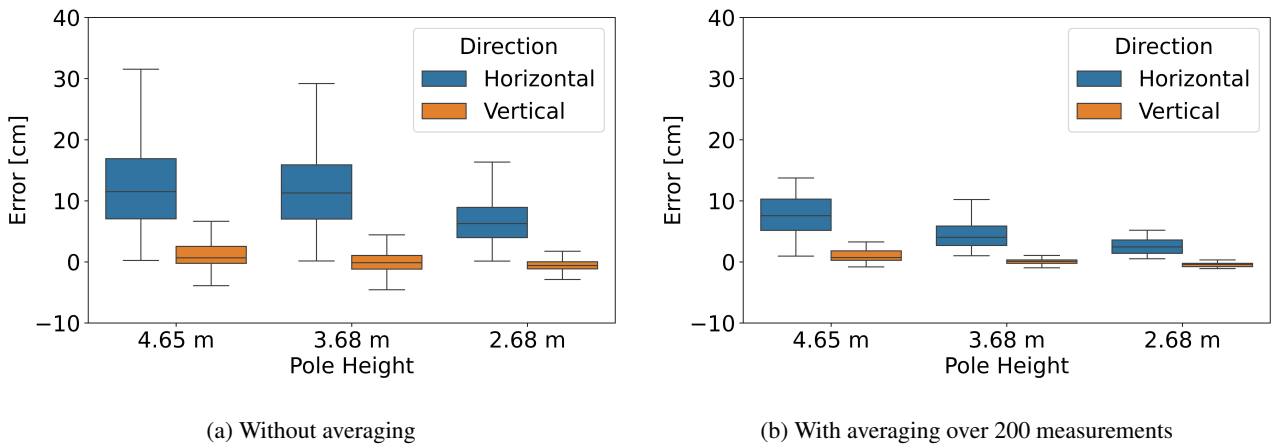


Figure 2. Boxplot of measurement errors of our experimental evaluation.

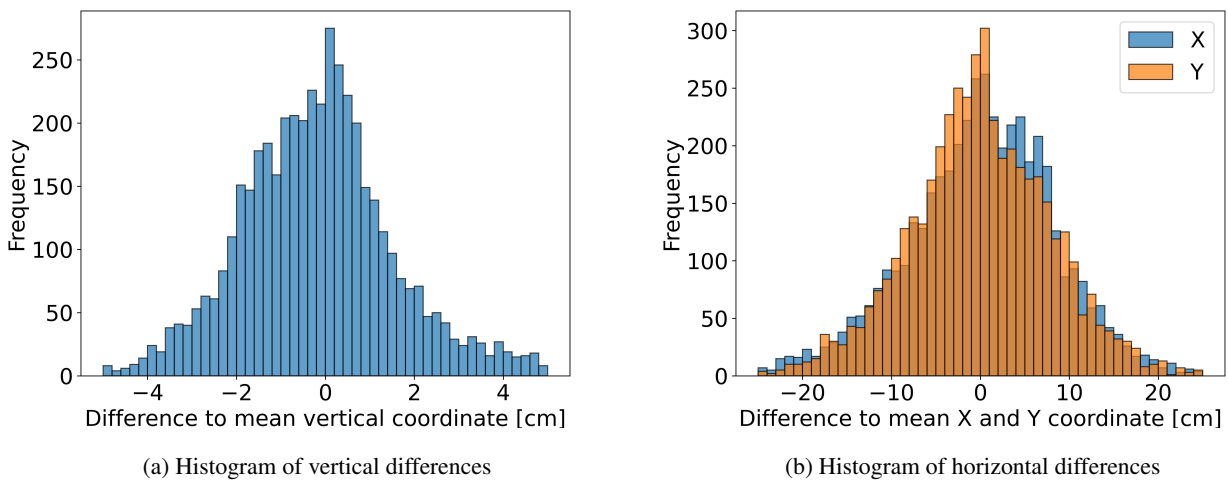


Figure 3. Histograms of single measurement differences for 4.65 m pole length from in-air evaluation.

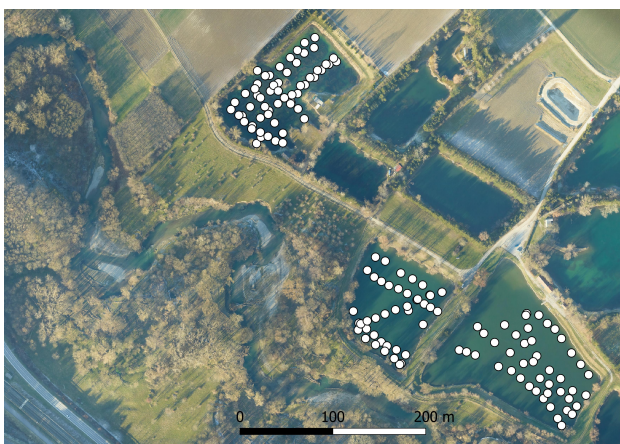


Figure 4. Test site of our field trial near Loosdorf, Austria (48.2166 N, 15.3744 E).

The standard deviations (Equation 4) derived from these distributions are at 1 cm (vertical) and 2.7 cm (euclidean horizontal), respectively, for a single measurement. We see that these values are two to three times smaller than for the experimental evaluation. Here, we assume the stabilisation of the measurement pole by the water column to be the main reason. Analogously to the experimental evaluation, we can additionally analyze the distance between both reflectors on the dual-prism pole. For our field test, it shows a lower standard deviation than for the experimental evaluation of 2.5 mm at pole length 4.65 m, although the measurement distance increases up to 150 m, which theoretically decreases the measurement accuracy.

From the field test, we can also derive statistics regarding the avoided errors when using the tilt-compensating dual-prism pole. With water depths ranging from 1.5 to 5 m, measurement by canoe or a similar vehicle is a good solution to survey water bodies. However, stable positioning of a canoe is difficult, not only when considering the necessary time to complete stopping and maintaining the position, but also with regard to wind or currents pushing the boat. Thus, the top part of the pole, held by a surveyor, moves relative to the static bottom part. For our field test, we find that the pole inclination ranges between  $0^\circ$  and  $25^\circ$  on all measurements, with most measurements occurring between the  $10^\circ$  and  $15^\circ$  inclination. The height error



Figure 5. Photograph during data acquisition at our test site. Two Leica MS60 are controlled using a Laptop and Raspberry Pi, the bathymetric points are measured by a team of two in a canoe.

caused by this inclination strongly depends on the pole length used. However, for a pole length of 4.65 m the height error avoided by our tilt-compensating dual-prism pole amounts to 7 cm to 16 cm (tilt between 10-15°).

## 5. Discussion

In this section, we focus on the discussion of our results and highlight challenges we encountered during the construction and testing of our tilt-compensating dual-prism pole.

### 5.1 Achievable uncertainty for bathymetric reference data

In Section 4, we described the theoretical uncertainty and the empirically determined uncertainty of the tilt-compensating dual-prism pole. We can see a small difference between the expected and observed height uncertainties. The empirically observed height RMSE of a single measurement is 2.7 cm, based on our experimental evaluation. This matches well with the variance propagation, which yields an expected standard deviation of about 2 cm. However, after averaging, the height RMSE reduces to 1.6 cm and rejecting strongly tilted measurements reduces it further to 0.9 cm. The Euclidean horizontal RMSE is around 8 cm and thus much higher than the theoretically estimated value. It is difficult to interpret these height uncertainties, as there are no data on the achievable accuracy of tilted measurements based on RTS with pole heights of 4.65 m. However, conventional measurements with 2 m pole height and RTS reach standard deviations four times smaller than for our pole at 2.68 m length (Table 1: 7 mm), of less than 2 mm (Leica

Geosystems AG, 2016). According to the manufacturer's data sheet, commercially available tilt-compensated measurement poles, based on IMU data, are of similar accuracy. For example, the Leica AP20 reaches a typical uncertainty of 11 mm for the horizontal position and 2 mm for the vertical position (Maar, 2022) at 2 m height for a tilt of 10°. However, GNSS-RTK height measurements are usually less accurate, even for short pole lengths, reaching only 2 cm to 5 cm standard deviation depending on the source of the uncertainty assessment for GNSS-RTK (Wiener Netze GmbH & Co KG, 2024; Luo et al., 2018b; Hexagon AB, 2022; Trimble Inc, 2024). Based on our practical accuracy assessment, we can state a height RMSE of 2 cm and an Euclidean, positional RMSE of about 8 cm for our system for 4.65 m pole length. With better accuracy, reaching 1 cm height RMSE and 3 cm euclidean, horizontal RMSE for a shorter pole length of 2.68 m.

In addition to the experimental uncertainty assessment, the conducted field test allows us to have a realistic assessment of our method. In Figure 3 and 6, we see that the spread of the position data within a measurement window during the underwater measurements is two to three times smaller than during our experimental evaluation without water. This indicates that our experimental evaluation overestimates the uncertainty of the position measurement. Apparently, the behaviour of the measurement pole differs greatly between the air and underwater environment. This is most likely caused by the dampening effect of the water column and the stabilisation point at 4.65 m pole height due to the hand holding the pole. Thus, we assume that the actual measurement accuracy of the horizontal component is significantly higher than 8 cm RMSE and can be estimated by the standard deviation during a measurement window which amounts to 1 cm for the vertical and 2.7 cm for horizontal component. This matches well with our propagated, theoretical uncertainties.

In general, our method provides a feasible option for acquiring accurate bathymetric reference data, which is essential for the evaluation of LiDAR and SONAR data, as this data can hardly be acquired by other methods with similar accuracy.

### 5.2 Deformation of the measurement pole

Another topic to address is the deformation of the measurement pole. As already mentioned, we assume a different behaviour of the pole for air and water environments. For our study, we selected a telescopic measurement pole that combines lightweight and thus ease of use with a large pole length. As a standard product from a surveying shop, it is affordable. However, when completely extended, it shows a deformation of up to 10 cm when put under strong force in the middle. This deformation is stronger for the thinner, upper telescope elements than the thicker, lower elements. Also, the extension segment that builds up the baseline between both prisms shows additional deformation when the pole is tilted. This deformation appears stronger for our experimental evaluation, where the pole is held at about 1.3 m height, leaving more than 4 m of the pole unstabilized. For our field test, where the pole is held 1.3 m from the top and the movement of the submerged part is damped by the water column, we see an increased accuracy for the underwater application. Thus, it is difficult to answer how much this deformation or instability affects the measurement uncertainty. We modelled the deformed pole as a parabola to assess the effect of this deformation on the height measurement. With maximum deformations of 3, 6 or 9 cm the height is measured 2, 8

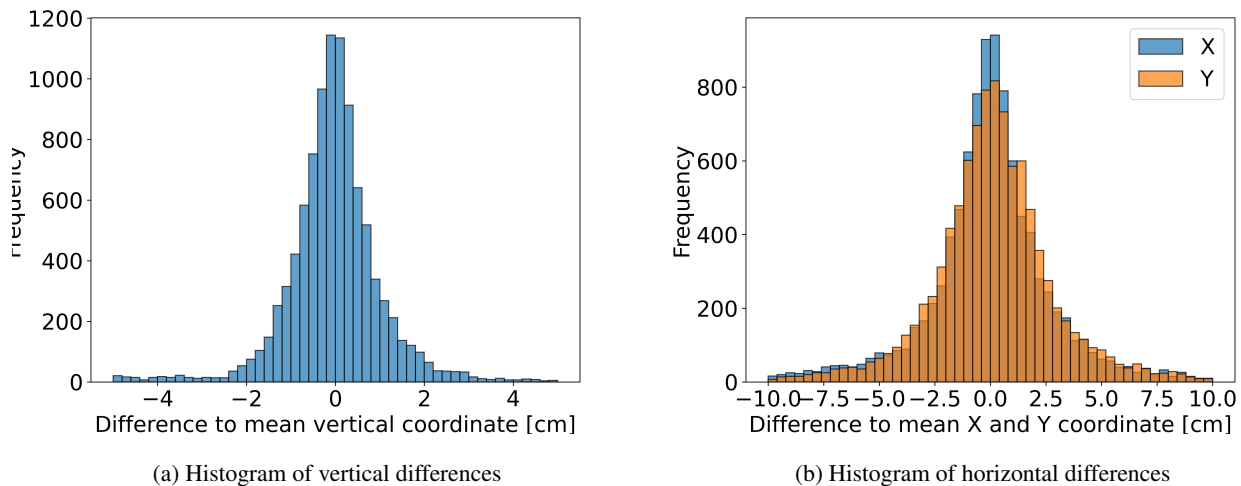


Figure 6. Histograms of single measurement differences from in-water measurements.

or 17 mm too small. However, the occurrence of pole deformation during the measurement, in particular when the pole is submerged, is uncertain. Our field study took place in standing water, and the only acting force on the pole was the surveyor. Thus, we believe the deformation of the pole itself to be insignificant. However, for water bodies with currents, e.g. rivers, the deformation might become significant. There, the acting force can be simulated based on the flow velocity, and the potential deformation of the pole can be estimated. Another solution is to minimize the deformation by using a more rigid measurement pole. Regarding the potential deformation of the baseline segment between both prisms, any error in this baseline segment is strongly amplified when propagating the vector over the whole pole length. This can have a significant impact on the measurement. However, we again believe this effect to appear stronger during our experimental evaluation than during field measurements, where the majority of the pole is submerged. Nevertheless, the possible deformation of the pole itself and the baseline segment serves as a trigger to improve our pole and use a more rigid mounting of the prisms and measurement pole.

### 5.3 Suitability of different RTS models

During our research, we found other RTS models, e.g. the Leica TS16, to be inadequate for measurements using the dual-prism pole. The occurrence of two reflectors in the field of view of the Leica TS16 led to incorrect measured points, meaning a non-existent point between both reflectors was measured. This effect was strongly related to (i) the spacing between both prisms and (ii) the distance between the RTS and the prism. However, this non-existent point made up about a third of the total measurements but was evenly distributed over the 10 s time window. By introducing strong filtering and eliminating the measurements towards the non-existent point, we were still able to use the data acquired with the TS16. In addition, the target tracking performance of the TS16 led to many more prism mix-ups and loss-of-lock situations than with the MS60. After introducing strict filter criteria, the TS16 data appears to have similar accuracy as the MS60 data. However, when using different RTS models, the estimation and correction of the intrinsic latency between distance and angle measurements of the RTS, should be considered. Thus, we advise conducting careful testing of RTS models before applying them for kinematic dual-prism pole measurements.

### 5.4 Relation of pole tip to bathymetry

Perhaps the largest source of uncertainty in the acquisition of bathymetric reference data is not the determination of the measurement pole tip but the relation between the pole tip and the actual bathymetry. SONAR, LiDAR, and the measurement pole all have the ability to penetrate the sediment to a certain extent, leading to different interpretations of the bathymetry. One of the first things to discuss is the submersion of the pole tip in sediment. For soft sediment, this can easily cause several centimetres of error. Thus, our pole uses a circular disk instead of a tip to minimize the sediment submersion of the pole. However, this disk also compresses any occurring vegetation or rests on stones, resulting in a potentially too high measurement. For the acoustic and optical waves of SONAR and LiDAR, it is hard to quantify the sediment penetration, but it is well known that they penetrate sparse vegetation. Thus, the three different techniques might exhibit discrepancies solely based on their vegetation and ground penetration characteristics.

Another error source is the impact of sloping terrain on the circular disk on the measurement pole and its interaction with the footprints of SONAR and LiDAR. For the remote sensing techniques, this largely depends on the footprint size and processing algorithms, and for the pole measurement, it is very dependent on the disk size, surveyor, and sediment. Therefore, we omit a detailed discussion at this time and rather outline this as a future research direction.

## 6. Conclusion and Outlook

In our study, we present the concept of a tilt-compensating dual-prism measurement pole that allows slight movement of the pole as well as tilt-compensated measurements. The tilt compensation allows very long pole lengths and measurements from moving platforms, which, in turn, enables bathymetric reference measurements in large water depths. Theoretically, the water depth is only restricted by the length of the measurement pole. The pole used in this study is 4.65 m long, allowing the measurement of shallow water bodies as a reference for bathymetric LiDAR and SONAR data. The measurement pole features two reflectors, which are each continuously measured for 10 s by two time-synchronized RTS. The measured coordinates

of both reflectors allow the estimation of a tilt vector and the propagation of the vector onto the foot of the pole, i.e. the bathymetric ground point. However, the setup requires a line-of-sight between both RTS and the measurement pole, which can drastically increase the operational effort, and is limited to approximately 150 m measurement distance, due to the closeness of the reflectors on the pole (about 1.2 m).

We present our realization of this setup and perform an uncertainty assessment based on variance propagation and an experimental evaluation. We see, based on our experimental in-air evaluation, that measurements of bathymetric reference data in 4 m to 5 m deep water are possible with a height RMSE of 1 cm and position RMSE of about 8 cm. However, we see better results for shorter pole lengths, indicating a strong dependence between pole length and measurement uncertainty. In addition, our in-water field test suggests that the dampening effect of the water column on the pole decreases any deformation or instability of the pole and thus increases our position measurement accuracy by a factor of two to three. We can support this with the results of our field test, where the standard deviations within each 10 s measurement window reach values of 1 cm for the vertical and 2.7 cm for the euclidean horizontal component. We also highlight the strengths and weaknesses of our approach and point out the challenges in relating bathymetric ground measurements to remote-sensing techniques. In general, our contribution addresses the important issue of reference data in shallow water bathymetry for both LiDAR and SONAR.

Our approach can be used to obtain accurate reference data for bathymetry based on SONAR and LiDAR in shallow water bodies. The reference data can be used to reliably assess the uncertainty of bathymetric sensors and allows the accurate stochastic modelling of these sensors.

## References

- Bangen, S. G., Wheaton, J. M., Bouwes, N., Bouwes, B., Jordan, C., 2014. A methodological intercomparison of topographic survey techniques for characterizing wadeable streams and rivers. *Geomorphology*, 206, 343-361.
- Gojcic, Z., Kalenjuk, S., Lienhart, W., 2018. A routine for time-synchronization of robotic total stations. *AVN. Allgemeine Vermessungsnachrichten*, 125(10), 299–307.
- Grimm, D., Hornung, U., 2015. Leica AT-Rplus–Leistungssteigerung der automatischen Messung und Verfolgung von Prismen. *AVN - Allgemeine Vermessungsnachrichten*, 8–9.
- Grimm, D., Kleemaier, G., Zogg, H.-M., 2015. ATRplus White Paper.
- Hexagon AB, 2022. HxGN SmartNet Services.
- International Hydrographic Organization, 2022. Standards for Hydrographic Surveys S-44 Edition 6.1.0.
- Kälin, U., Staffa, L., Grimm, D. E., Wendt, A., 2022. Highly Accurate Pose Estimation as a Reference for Autonomous Vehicles in Near-Range Scenarios. *Remote Sensing*, 14(1), 90. Multidisciplinary Digital Publishing Institute, <https://doi.org/10.3390/rs14010090>.
- Leica Geosystems AG, 2016. Leica MS60/TS60 User Manual.
- Leica Geosystems AG, 2025. Leica CoastalMapper Superior bathymetric efficiency.
- Luo, X., Schaufler, S., Carrera, M., Celebi, I., 2018a. High-precision RTK positioning with calibration-free tilt compensation. *Proceedings of the FIG Congress*, 1–17.
- Luo, X., Schaufler, S., Richter, B., 2018b. Leica GS18 T World's Fastest GNSS RTK Rover.
- Maar, H., 2022. Leica AP20 AutoPole: Advancing Productivity in Total Station Workflows White Paper. Leica Geosystems AG.
- Mandlbürger, G., 2022. A Review of Active and Passive Optical Methods in Hydrography. *The International Hydrographic Review*, 28, 8-52. <https://doi.org/10.58440/ihr-28-a15>.
- Menna, F., Nocerino, E., Calantropio, A., 2024. High-accuracy height differences using a pressure sensor for ground control points measurement in underwater photogrammetry. *The International Archives of the Photogrammetry, Remote Sensing and Spatial Information Sciences*, XLVIII-2-2024, 273-279. Copernicus, <https://doi.org/10.5194/isprs-archives-XLVIII-2-2024-273-2024>.
- Norbit Subsea, 2021. Norbit Winghead i77h.
- Riegl Laser Measurement Systems GmbH, 2021. Riegl VQ-840-G.
- Stempfhuber, W., Sukale, J., 2017. Kinematische Leistungsfähigkeit der Multistation Leica MS60. *Geomatik Schweiz*.
- Thalmann, T., Neuner, H., 2021. Temporal calibration and synchronization of robotic total stations for kinematic multi-sensor-systems. *Journal of Applied Geodesy*, 15(1), 13–30. De Gruyter, <https://doi.org/10.1515/jag-2019-0070>.
- Thalmann, T., Neuner, H., 2024. Sensor fusion of robotic total station and inertial navigation system for 6DoF tracking applications. *Applied Geomatics*. Springer, <https://doi.org/10.1007/s12518-024-00593-4>.
- Tombrink, G., Dreier, A., Klingbeil, L., Kuhlmann, H., 2023. Trajectory evaluation using repeated rail-bound measurements. *Journal of Applied Geodesy*, 17(3), 205–216. De Gruyter, <https://doi.org/10.1515/jag-2022-0027>.
- Trimble Inc, 2024. Trimble R980 GNSS SYSTEM.
- Vogel, S., van der Linde, M., Hake, F., 2023. Development and Validation of an External GPS Time Synchronization for Robotic Total Station Control. *Ingenieurvermessung 23. Beiträge zum 20. Internationalen Ingenieurvermessungskurs Zürich, 2023*, 181–194. Wichmann.
- Wiener Netze GmbH & Co KG, 2024. Bedingungen über die Nutzung von EPOSA.